Experimental and Numerical Study on Phase Change Material (PCM) for Thermal Management of Mobile Devices

Yusuke TOMIZAWA[*1], Katsuhiko SASAKI[*2], Akiyoshi KURODA[*2], Ryo TAKEDA[*2] and Yoshihiko KAITO[*3]

[*1] Graduate School of Engineering, Hokkaido University, Kita 13, Nishi 8, Kita-ku, Sapporo, Hokkaido 060-8628, Japan

[*2] Faculty of Engineering, Hokkaido University, Kita 13, Nishi 8, Kita-ku, Sapporo, Hokkaido 060-8628, Japan

[*3] Fujitsu Limited, Kita 7, Nishi 4-3-1, Kita-ku, Sapporo, Hokkaido 060-0807, Japan

*Corresponding Author:

Katsuhiko SASAKI, Ph.D
Professor, Faculty of Engineering, Hokkaido University
Kita 13, Nishi 8, Kita-ku, Sapporo, Hokkaido 060-8628, Japan
Tel/Fax: +81-011-706-8376, E-mail:katsu@eng.hokudai.ac.jp

Keywords: Phase Change Material (PCM), Thermal management, Passive cooling, Mobile device, Finite element method (FEM)

***Word count*:** 4060 words (Introduction through Conclusion)

***Manuscript Type*:** Research Paper

Abstract

As mobile devices become more complex and higher in performance despite the smaller in size, heat concentration at localized areas has become a problem. In recent years, passive cooling using phase change materials (PCMs) have drawn attention as thermal management methods for mobile devices. PCMs reduce the temperature increase rate due to their latent heat properties. This reduction in the temperature increase rate is called a “delay effect”. Moreover, microencapsulated PCMs (MPCMs) are attracting attention because they keep the melted PCMs from leaking. In this study, PCM sheets containing MPCM/polyethylene composite material are investigated for the thermal management of mobile devices. Namely the authors conduct a series of experiments using the PCM sheet with high thermal conductivity sheet mounted into a simply modeled mobile device. Effects of the mass, the latent heat, the thermal conductivity, the configuration of the PCM sheet, and high thermal conductivity sheet on the temperature of a smart phone simulator are investigated. A finite element analysis (FEA) is also conducted considering the phase change of PCMs to investigate the optimal dimension and shape of PCMs. As a result, the delay effect of PCMs and effectivity of a copper sheet pasted on the PCMs are verified by experiments. Moreover, FEA shows that using the PCM sheet with high thermal conductivity sheet has an advantage for the thermal management of mobile devices and gives an optimal condition of the PCM sheets.

1. Introduction

In recent years, complex and high-performance mobile electronic devices such as smart phones and tablet PCs have been spreading widely. However, the power density of these devices has become higher and the heat dissipation area smaller [1]. This will eventually lead to overheating and damage the components on the substrate due to the acceleration of the thermal fatigue in the solder [2]. In addition, high surface temperature of the mobile devices will lead to discomfort during usage [3]. Thus, thermal management of mobile devices is quite important.

Active thermal management using fans is a popular method for cooling electronic devices [4]. However, mobile electronic devices do not have enough space to insert fans or heat sinks [5]. In addition, fans are inadequate for use with mobile devices due to noise, maintenance, and additional power consumption [6]. Therefore passive thermal management is widely chosen as the cooling method of mobile devices. Phase change materials (PCMs) have attracted a lot of attention for high efficient passive cooling functions of mobile devices. As PCMs absorb heat at a constant temperature due to their latent heat during melting process, the temperature increase rate of PCMs decreases, which is called a “delay effect” in this paper. This suggests that there is a possibility of controlling the surface temperature of the mobile devices by using PCMs.

The thermal management of electronic devices using PCMs has been studied by many researchers. For example, Alawadhi and Amon conducted experimental and numerical studies on PCM thermal control unit (TCU) for portable electronic devices and showed the effects of the power operation and the Stefan number [7]. Tan *et al.* carried out a series of experiments using heat storage unit (HSU) and heat sink filled with PCM and clarified the effect of heat distribution [8], number of fins in the heat sink [1,6], the power levels [6], and steady and transient state heating conditions [1]. Numerical simulations were also performed to study the effects of power levels, number of fins, fin height, and fin thickness [9]. Ishizuka *et al.* conducted numerical simulation of electronic devices including PCM with thermal network method [10-12]. Kandasamy *et al.* carried out experiments of PCM package for thermal management of portable electronic devices to investigate the effect of power input, orientation of package, and various melting/freezing times [13]. They also conducted both experimental and numerical investigation of PCM-based heat sink for thermal management of

transient electronic devices to reveal the effects of power level and designs of heat sinks [14]. Mahmoud *et al.* experimentally investigated the effects of heat sink configuration, power level, and PCM type for PCM based heat sinks [15]. Qu *et al.* studied the heat sink with copper metal foam–paraffin composite [16]. Passive cooling system using PCM for high-powered Li-ion battery package was investigated by Kizilel *et al.* [17] and Li *et al.* [18]. As shown above, almost all studies focused on relatively large size devices such as heat sinks and Li-ion battery packages, and there are few research works to verify the applicability of PCMs to mobile devices.

In order to apply PCMs to mobile devices, it is necessary to seal PCMs to prevent melted PCMs from leaking. Recently, studies on microencapsulated PCMs (MPCMs), in particular, MPCM composite materials have been carried out. The advantages of MPCMs are preventing the liquid PCM leakage and adapting various materials for heat storage by compounding MPCMs into various materials. Yoshinori *et al.* measured thermophysical properties of composite materials containing silicon rubber and MPCMs [19]. Katsuragi *et al.* conducted experiments under unsteady heat conduction and also verified the effect of the composites by a numerical simulation model [20]. Wang *et al.* fabricated phase change composites containing MPCMs, expanded graphite, and high density polyethylene. They clarified the thermal conductivity enhancement of the composites [21]. Zhang *et al.* investigated the melting thermal performances of MPCM composite plate containing carbon fibers, aluminum powder, and silica aerogel [22]. The physical properties of the MPCM composites have been also studied by some researchers [23-29]. However, the understanding of thermophysical properties of MPCM composites is not sufficient. This means that it is difficult to obtain optimal conditions for thermal control using PCMs by numerical simulation.

In this study, the authors fabricate an experimental system simulating a mobile smart phone. The system contains substrate, heater, case, and sheets made of MPCM/polyethylene composite. Both experimental and numerical investigations are conducted to verify the applicability of PCMs to the thermal management of mobile devices. First, experiments to clarify the mass effect of PCM sheet on the temperature change are carried out using the experimental system. Afterwards, experiments to investigate the effects of latent heat, thermal conductivity, and configuration of the PCM sheets on the temperature change are also carried out. Moreover, a copper sheet, as a high thermal conductivity

material, is incorporated in the experimental system and the effect of a copper sheet on the phase change of the PCM sheet is revealed. Finally, numerical simulations to estimate the thermophysical properties of the MPCM/polyethylene composite are conducted using finite element method (FEM).

2. Experiment on Thermal Characteristic of PCM Sheets

2.1 Experimental method

2.1.1 PCM sheet

Paraffin is used as the PCM in this study. Paraffin has higher latent heat than other PCMs such as organic salt and inorganic salt. The PCM is microencapsulated by melamine resin to prevent the melted paraffin from leaking. The MPCM can be applied to the mobile devices such as smart phones because of its leak-proof characteristic. PMCD-32SP (Miki Riken Industrial Co., Ltd.) is chosen as the MPCM for this study. The physical properties of the MPCM are shown in Table 1. As shown in Fig. 1(a), since the MPCM is in powder form, the MPCM is ordinary used as master batches made by combining 50wt% polyethylene and 50wt% MPCM, shown in Fig. 1(b).

Figure 2 shows a metal mold used to make the PCM sheets. First, the mold is put on a hot plate and heated up to 150°C. After that, the MPCM master batch is put into the mold and a stainless steel plate is set on the master batch with 40 N load. Finally the PCM sheet can be obtain after cooling the mold. In this procedure, three different types of the mass of PCM sheets are prepared. Figure 3 shows a photo of the PCM sheet. The size and mass of the PCM sheets are shown in Table 2.

2.1.2 Experimental procedure

Figure 4 shows the main test part in this experiment. The case in Fig. 4 is made of 1 mm thick polycarbonate boards and the size of the case is 122 mm length, 62 mm width, and 11 mm height, respectively. The PCM sheet is put on a rubber heater and they are also put on a heat insulator covered by the case. T-type thermocouples are used to measure the temperature. Three thermocouples are attached to the heater, the PCM sheet, and the case as shown in Fig. 4(b). The thermocouples for the PCM sheet and the case are inserted into small grooves with epoxy resin to fill the clearance. Kapton tape is then used to fix the thermocouples firmly. No special grooves are

prepared on the surface of the heater and only kapton tape is used to attach the thermocouple. An additional thermocouple is used to measure the ambient temperature. The thermocouples used were calibrated within the range of 0-100°C and have an uncertainty of 0.5°C.

A power supply is used to give accurate power of 2.00 W to the heater. The temperatures at each point are measured just after heating starts. The measurements of the temperatures are conducted every minute during 90 minutes of heating. The experiment is conducted three times under the same experimental condition. Four experimental conditions are chosen; no PCM sheet, PCM sheet A (5.10 g), PCM sheet B (7.22 g), and PCM sheet C (9.86 g).

2.1.3 Experimental data processing

In order to remove the influence of the ambient temperature variation, a value of temperature rise is used as the value to evaluate the thermal characteristic of the PCM sheet. The temperature rise is defined as the difference between the measured temperature and the ambient temperature. In addition, values of maximum temperature rise and saturation time are used for the evaluation. The value of saturation time means the time until the temperature becomes a constant value.

To determine the maximum temperature and the saturation time, noise of the measurement is reduced as follows. The following fitting function of $\Delta T_f(t)$ is used,

$$\Delta T_f(t) = A_1 \operatorname{erf}(B_1 t) + A_2 \operatorname{erf}(B_2 t) + A_3 \operatorname{erf}(B_3 t) + C \tag{1}$$

$$\operatorname{erf}(t) = \frac{2}{\sqrt{\pi}} \int_0^t e^{-\tau^2} \mathrm{d}\tau \tag{2}$$

where A_1, A_2, A_3, B_1, B_2, B_3 and C are fitting constants, and erf(t) is Gauss error function. Figure 5(a) shows an example of fitting curve of the case temperature without PCM sheet, and Fig. 5(b) with PCM sheet C (9.86 g). Figure 5 also shows the definitions of both the maximum temperature rise ΔT_{max} and the saturation time t_{sat}. These values are obtained by using the fitting curves.

2.2 Experimental results and discussion

Figure 6 shows the relationship between the value of temperature rise and time of no PCM sheet,

PCM sheet A (5.10 g), B (7.22 g) and C (9.86 g). Figure 6(a) shows the heater temperature and Fig. 6(b) the case temperature. The PCM sheet affects the temperature variation: the inflection parts of the temperature rise variation can be seen as shown in Fig. 6 by a circle. While the PCM is melting, the polyethylene composing the PCM sheet conducts heat. Therefore, the period in which the temperature remains relatively constant does not appear. However, decrease in the temperature increasing rate is shown clearly, which indicates the effect of the PCM. Moreover, the temperature rise rates with the PCM sheet are slower than that without the PCM sheet. Namely, the PCM sheets lead to the delay effect due to their latent heat.

The PCM sheets increase the temperature rise of the heater as shown in Fig. 6(a). On the other hand, the PCM sheets decrease the temperature rise of the case as shown in Fig. 6(b). The reason of the countertrend between the temperatures of the heater and the case is because the thermal resistance between the heater and the case with the PCM sheet is larger than that without the PCM sheet. That is, the PCM sheet suppresses the generation of natural convection and the heat transfer in the inner air.

As for the effect of the mass of the PCM sheet on temperature, the mass of the PCM sheet affects temperature as shown in Fig. 6. The temperature rise of the heater becomes lower with increase in the mass of the PCM sheets. As shown in Table 2, the thickness of the PCM sheets increases and the thickness of the layer of the inner air decreases with increase in the mass of the PCM sheets. Most of heat is transferred by thermal conduction in the inner air. Therefore, the overall thermal resistance decreases with decrease in the thickness of the layer of the inner air and with increase in the thickness of the PCM sheets.

Figure 7 shows the relationship between the mass of the PCM sheets and the saturation time. The symbols show the average of three times of experiment. The saturation time increases with increase in the mass of the PCM sheets as shown in Fig. 7. The larger delay effect can be seen with increase in the mass of the PCM sheets. A linear relationship between the mass of the PCM sheets and the saturation time can be also seen in Fig.7.

3. Experiment on Application of PCM Sheets to Smart Phone Simulator

3.1 Experimental procedures

3.1.1 Preparation of modified PCM sheets and a PE sheet

Considering actual used conditions of mobile phones, a small mold is used to modify the PCM sheets for the conditions. To clarify the effect of the latent heat of the PCM sheet, a polyethylene sheet (PE sheet) is also made and compared with the PCM sheets. The polyethylene powder (SUNFINE^{TM} XLH451) is used for the PE sheet. Figure 8 shows the equipment to mold the PCM and the PE sheet. The steel mold serves as the punch guide to provide uniform thickness to the sheets. The strong magnet is used to prevent leakage of the melted PCM master batch or PE powder from the space between the mold and the aluminum plate. The PCM master batch or the PE powder is set into the mold, and pressured by a punch in an electric furnace set at 155°C. Two PCM sheets in different size of 25 × 25 × 4 mm and 50 × 50 × 1 mm, and a PE sheet of 25 × 25 × 4 mm are made for the experiments. The PCM sheets of 25 × 25 × 4 mm and 50 × 50 × 1 mm have the same volume. Figure 9 shows photos of the PCM sheets of 25 × 25 × 4 mm and 50 × 50 × 1 mm. PCM sheets lined with copper sheets are prepared to clarify the advantage to use PCM sheets with high thermal conductivity materials for mobile phones.

3.1.2 Experimental setup

Figure 10 shows a schematic diagram of the test section in the experiment. The front case is made of polycarbonate boards and the rear case of acrylic board. A ceramic heater for simulating LSI is fixed on a substrate by a double-sided thermal tape. A PCM (PE) sheet is also fixed on the heater by the thermal tape. When the PCM sheets lined with copper sheets are used, the copper sheets are attached to the heater. Namely, the copper sheet is situated between the heater and the PCM sheet. Nine thermocouples are attached to the heater, the PCM (PE) sheet, the substrate, the front case, and the rear case as shown in Fig. 10(b). An additional thermocouple is used to measure ambient temperature.

The voltage of 8.5 V is applied to the heater, and the temperatures are measured just after the heating starts. The power of the heater becomes 1.3 W in steady state. Temperatures are measured for 60 minutes during heating. Experiments are conducted three times with the same condition.

3.2 Experimental results and discussion

Figure 11 shows the relationship between the value of the temperature rise and time. Solid circles, solid diamonds, solid triangles, solid squares, open triangles, and open squares show the results of no sheet, PE sheet (25 × 25 × 4 mm), PCM sheet (25 × 25 × 4 mm), PCM sheet (50 × 50 × 1 mm), PCM sheet (25 × 25 × 4 mm) lined with copper sheet, and PCM sheet (50 × 50 × 1 mm) lined with copper sheet, respectively. Figure 11(a) shows the heater temperature and Fig. 11(b) the case temperature. Figures 12 and 13 show the maximum temperature rise and the saturation time in all test conditions, respectively. The temperature rise rate of the thick PCM sheet (25 × 25 × 4 mm) is slower than that of the thin PCM sheet (50 × 50 × 1 mm) in spite of the same mass as shown in Fig. 11. Furthermore, the temperature rise rate of the PCM sheets lined with copper sheets is slower than that of the PCM sheets without copper sheets.

Focusing on the results of no sheet, PE sheet (25 × 25 × 4 mm), and PCM sheet (25 × 25 × 4 mm) to clarify the effects of latent heat and thermal conductivity of the PCM in Fig. 12, the temperature rise of the heater decreases by using the PCM (PE) sheet. Since the thermal conductivity of the PCM sheet is higher than that of the PE sheet, the PCM sheet leads to higher temperature rise of the heater than the PE sheet. Therefore, when replacing the inner air of the mobile devices with the PCM sheet, the temperature of the LSI decreases. However, when replacing the resin components of the mobile devices with the PCM sheet, the temperature of the LSI increases. As for the saturation time shown in Fig. 13, the PCM sheet gives longer saturation time than the PE sheet. The PCM used in this study has the same heat capacity as polyethylene. Therefore, the latent heat of the PCM has a larger effect on the saturation time than the sensible heat.

The size effect of the PCM sheet on temperature is discussed comparing the results of two PCM sheets of the same volume (same latent heat) but different size (25 × 25 × 4 mm and 50 × 50 × 1 mm). The saturation time of the thick PCM sheet (25 × 25 × 4 mm) is longer than that of the thin PCM sheet (50 × 50 × 1 mm) as shown in Fig. 13. Thus, the thickness of the PCM sheet has a large effect on the saturation time. Therefore, when applying the PCM sheets in mobile devices, thicker PCM sheets are more effective for the thermal design of mobile devices.

To discuss the effect of copper sheet on the temperature, the comparison between the results of two PCM sheets (25 × 25 × 4 mm and 50 × 50 × 1 mm) lined with copper sheet is conducted. The copper sheet decreases the temperature rise of the heater as shown in Fig. 12. By using the copper foil, the temperature rise of the front case increases when the thick PCM sheet (25 × 25 × 4 mm) is used, and decreases when the thin PCM sheet (50 × 50 × 1 mm) is used. This means that the uniform temperature of the PCM sheet caused by the copper sheet leads to the large effect of the PCM on the temperature rise. As for the saturation time, the thick PCM sheet gives longer saturation time as shown in Fig. 13. Therefore, the PCM sheet lined with high thermal conductivity materials such as copper sheet has an advantage in use with the mobile phones.

4. Numerical Simulation

4.1 FE model

In this study, the thermal fluid analysis considering the phase change of PCM is performed by using ANSYS Fluent in commercial FEM analysis software ANSYS 14.5 (ANSYS, Inc.). Figure 14 shows a finite element (FE) model including a front case, a rear case, a substrate, a PCM (PE) sheet, inner air, and nuts and bolts to fix the substrate. Total number of nodes and elements is 93196 and 317388, respectively. The FE model is made to reproduce the experimental setup.

The enthalpy-porosity method is used to express the phase change of the PCM sheets. The enthalpy of the PCM sheet is represented by the sum of the sensible enthalpy and the latent enthalpy. The latent enthalpy ΔH is provided by following equation,

$$\Delta H = \beta L \tag{3}$$

where β and L is the liquid fraction and the latent heat of the material, respectively. The liquid fraction β is equal to zero when the temperature is below the solidus temperature as the melting start temperature. The liquid fraction β is equal to one when the temperature is above the liquidus temperature as the melting finish temperature. The liquid fraction β is assumed to vary linearly in the temperature range of the solidus temperature to the liquidus temperature. Additionally, the surface-to-surface radiation model is used in order to express the radiation in the cases. The physical

properties used in this simulation are shown in Table 3. The physical properties of the PCM sheet are estimated by simple mixing rules shown in (4)-(6) and the Bruggeman equation shown in (7).

$$\rho = \rho_1\phi_1 + \rho_2\phi_2 \tag{4}$$

$$c_p = \frac{\rho_1 c_{p1}\phi_1 + \rho_2 c_{p2}\phi_2}{\rho} \tag{5}$$

$$L = \frac{\rho_1 L_1\phi_1 + \rho_2 L_2\phi_2}{\rho} \tag{6}$$

$$1-\phi = \left(\frac{k_p - k_c}{k_p - k_m}\right)\left(\frac{k_m}{k_c}\right)^{1/3} \tag{7}$$

where ρ, c_p, k and ϕ are the density, the specific heat, the thermal conductivity, and the volume fraction, respectively. The subscript numbers of 1 and 2 in (4)-(6) mean the material type. The subscript *m*, *p*, and *c* in (7) mean the matrix, the particle, and the compound, respectively. The physical properties of the PCM sheet are shown in Table 4. In addition, the viscosity of the PCM sheet is required because the phase change materials have to be treated as a fluid. In this simulation, the viscosity of the PCM sheet is provided with the value of 1 Pa·s. The value of 1 Pa·s was selected from the viewpoint of both calculation precision and calculation time.

4.2 Numerical conditions

The FE analysis is conducted for 60 minutes just after heating starts. The power of the heater is given the same value of 1.3 W as the experiment. The thermal contact resistances between the heater and the substrate, and between the heater and the PCM (PE) sheet are set to 15×10^{-4} m^2·K/W. The value is obtained by optimizing the temperature of each part comparing the simulation with experiments. The contact resistances include the thermal resistance of the thermal tape. The initial condition of the temperature is set to 19°C. The ambient temperature is also the constant value of 19°C. The heat transfer coefficients on the upper surface, the side surface, and the bottom surface of the cases are provided with 5.7 W/m^2·K, 6.0 W/m^2·K, and 3.7 W/m^2·K, respectively. The values were based on empirical laws of natural convection [30]. The emissivity of the surface of the cases is also

provided with 0.9 to express the heat dissipation from the surface of the case by both the convection and the radiation. The pressure-based coupled algorithm of ANSYS Fluent is selected to use the pressure-velocity coupling.

4.3 Numerical results and discussion

Figure 15 shows the comparison between the results of the solid model and the phase change model using the PE sheet. The solid, broken, and dot dash lines show the temperature rise variation of the heater, the PE sheet, and the front case, respectively. The difference between the results of the solid model and the phase change model are within 0.4°C. Therefore, reasonable numerical results can be obtained by considering the PCM sheet as the fluid material having the viscosity of 1 Pa·s.

Figure 16 shows the comparison between the numerical and the experimental results of no sheet, PE sheet, PCM sheet of 25×25×4 mm, and PCM sheet of 50×50×1 mm, respectively. In Fig. 16, solid and broken lines show numerical results of the heater and the front case, while diamonds and squares show the experimental results of the heater and the front case, respectively. The numerical results have good agreements with the experimental results as shown in Fig. 16. These results suggest that the physical properties of the MPCM/polyethylene composite can be estimated by using the mixing rules and Bruggeman equation. Therefore, optimal thermal design to apply the PCM sheets to the mobile phones may be easily conducted using the material properties obtained in the same way.

5. Conclusion

The aim of this paper was to investigate the application of PCM sheets to mobile phones. The thermal behavior of the PCM sheets was clarified using the smart phone simulator. The numerical simulations considering the phase change of the PCM sheet were also conducted by FE analysis. As a result, the following conclusions were obtained:

(1) The PCM sheets leads to the delay effect. Namely, the saturation time increases with increase in the mass of the PCM sheet, and there is a linear relationship between the mass of the PCM sheet and the saturation time.

(2) The latent heat of the PCM has a larger effect on the saturation time than the sensible heat.

(3) Since the thermal conductivity of the PCM sheet is higher than that of the PE sheet, the PCM sheet leads to higher temperature rise of the heater than the PE sheet, and also leads to lower temperature rise of the surface of the case than the PE sheet.

(4) The thickness of the PCM sheet has a large effect on the saturation time. Therefore, when applying the PCM sheets to the mobile devices, thicker PCM sheets are more effective for the thermal design.

(5) The copper sheet leads to low temperature rise and hardly affects the saturation time. Therefore, thick PCM sheets should be used alongside high thermal conductivity sheets.

(6) The estimation of the thermophysical properties of the MPCM composite by the mixing rules and Bruggeman equation can be adapted to simulate the heat transfer considering the phase change. This suggests that an optimal thermal design to apply the PCM sheets to the mobile phones may be easily conducted using the material properties obtained in the same way.

[Reference]

[1] G. Setoh, F.L. Tan, S.C. Fok, Experimental studies on the use of a phase change material for cooling mobile phones, International Communications in Heat and Mass Transfer, Vol.37 (2010), pp.1403-1410

[2] Y. Nishino, M. Ishizuka, S. Nakagawa, Study on the Enhancement of Natural Air Cooling Capability in the Vertical Channel Model of Compact Electronic Equipment (The Effect of the Clearance of a Channel on the Natural Cooling Capability) (in Japanese), Transactions of the Japan Society of Mechanical Engineers. B, Vol.75, No.755 (2009), pp.1479-1484

[3] Y. Shinki, S. Ubemoto, N. Kishimoto, D. Takeda, Y. Yamane, H. Miyoshi, The Thermal Design for Mobile Phones by Using Thermal Simulation System (in Japanese), Proceedings of Thermal Engineering Conference (2007), pp.219-220

[4] Z.Ling, Z.Zhang, G.Shi, X.Fang, L.Wang, X.Gao, Y.Fang, T.Xu, S.Wang, X.Liu, Review on thermal management systems using phase change materials for electronic components, Li-ion batteries and photovoltaic modules, Renewable and Sustainable Energy Reviews, Vol.31 (2014), pp.427-438

[5] Z. Luo, H. Cho, X. Luo, K.-i. Cho, System thermal analysis for mobile phone, Applied Thermal Engineering, Vol.28 (2008), pp.1889-1895

[6] S.C. Fok, W. Shen, F.L. Tan, Cooling of portable hand-held electronic devices using phase change materials in finned heat sinks, International Journal of Thermal Sciences, Vol.49 (2010), pp.109-117

[7] E.M. Alawadhi, C.H. Amon, PCM Thermal Control Unit for Portable Electronic Devices: Experimental and Numerical Studies, IEEE Transactions on Components and Packaging Technologies, Vol. 26 (2003), No. 1, pp.116-125

[8] F.L. Tan, C.P. Tso, Cooling of mobile electronic devices using phase change materials, Applied Thermal Engineering, Vol.24 (2004), pp.159-169

[9] S.F. Hosseinizadeh, F.L. Tan, S.M. Moosania, Experimental and numerical studies on performance of PCM-based heat sink with different configurations of internal fins, Applied Thermal Engineering, Vol.31 (2011), pp.3827-3838

[10] N. Fujii, M. Ishizuka, S. Nakagawa, Application of a thermal network method to the thermal analysis of electronic devices including phase change materials (in Japanese), In: Proceedings of the 44th Conference of The Japan Society of Mechanical Engineers Hokuriku Shin-etsu Branch (2007), pp.315-316

[11] N. Fujii, S. Takakuwa, M. Ishizuka, S. Nakagawa, Application of a thermal network method to the thermal analysis of electronic devices including phase change materials (in Japanese), In: Proceedings of the 45th Conference of The Japan Society of Mechanical Engineers Hokuriku Shin-etsu Branch (2008), pp.245-246

[12] S. Takakuwa, M. Ishizuka, S. Nakagawa, Application of a Thermal Network Method to Thermal Analysis of Electronic Device with Phase Change Materials: Modeling Technique of Latent Heat (in Japanese), In: Proceedings of the 46th Conference of The Japan Society of Mechanical Engineers Hokuriku Shin-etsu Branch (2009), pp.169-170

[13] R. Kandasamy, X.-Q. Wang, A.S. Mujumdar, Application of phase change materials in thermal management of electronics, Applied Thermal Engineering, Vol.27 (2007), pp.2822-2832

[14] R. Kandasamy, X.-Q. Wang, A.S. Mujumdar, Transient cooling of electronics using phase change material (PCM)-based heat sinks, Applied Thermal Engineering, Vol.28 (2008), pp.1047-1057

[15] S. Mahmoud, A. Tang, C. Toh, R. AL-Dadah, S.L. Soo, Experimental investigation of inserts configurations and PCM type on the thermal performance of PCM based heat sinks, Applied Energy, Vol.112 (2013), pp.1349-1356

[16] Z.G. Qu, W.Q. Li, J.L. Wang, W.Q. Tao, Passive thermal management using metal foam saturated with phase change material in a heat sink, International Communications in Heat and Mass Transfer, Vol.39 (2012), pp.1546-1549

[17] R. Kizilel, R. Sabbaha, J. R. Selmana, S. Al-Hallaj, An alternative cooling system to enhance the safety of Li-ion battery packs, Journal of Power Sources, Vol.194 (2009), pp.1105-1112

[18] W.Q. Li, Z.G. Qu, Y.L. He, Y.B. Tao, Experimental study of a passive thermal management system for high-powered lithium ion batteries using porous metal foam saturated with phase

change materials, Journal of Power Sources, Vol.255 (2014), pp.9-15

[19] K. Yoshinori, D. Katsuragi, J. Ogawa, H. Soeda, Unsteady Heat Conduction of Composite Materials Using Micro Encapsulated Phase Change Materials (MEPCM) (in Japanese), Proceedings of Thermal Engineering Conference 2007, pp.117-118

[20] D. Katsuragi, H. Soeda, Unsteady Heat Conduction of Composite Materials of Micro Encapsulated Phase Change Materials (MEPCM): Comparison of Experiment and Numerical Simulation (in Japanese), Symposium on Environmental Engineering (2009), pp.463-466

[21] X. Wang, Q. Guo, J. Wang, Y. Zhong, L. Wang, X. Wei, L. Liu, Thermal conductivity enhancement of form-stable phase-change composites by milling of expanded graphite, micro-capsules and polyethylene, Renewable Energy, Vol.60 (2013), pp.506-509

[22] J.J. Zhang, Z.G. Qu, Z.G. Jin, Experimental study on the thermal characteristics of a microencapsulated phase-change composite plate, Energy, Vol.71 (2014), pp.94-103

[23] J. Su, L. Ren, L. Wang, Preparation and mechanical properties of thermal energy storage microcapsules, Colloid and Polymer Science, Vol.284 (2005), pp.224-228

[24] J.-F. Su, L.-X. Wang, L. Ren, Z. Huang, Mechanical Properties and Thermal Stability of Double-Shell Thermal-Energy-Storage Microcapsules, Journal of Applied Polymer Science, Vol.103, pp.1295-1302

[25] J. Li, P. Xue, W. Ding, J. Han, G. Sun, Micro-encapsulated paraffin/high-density polyethylene/wood flour composite as form-stable phase change material for thermal energy storage, Solar Energy Materials & Solar Cells, Vol.93 (2009), pp.1761-1767

[26] J.-F. Su, S.-B. Wang, J.-W. Zhou, Z. Huang, Y.-H. Zhao, X.-Y. Yuan, Y.-Y. Zhang, J.-B. Kou, Fabrication and interfacial morphologies of methanol–melamine–formaldehyde (MMF) shell microPCMs/epoxy composites, Colloid and Polymer Science, Vol.289 (2011), pp.169-177

[27] J.-F. Su, X.-Y. Wang, Z. Huang, Y.-H. Zhao, X.-Y. Yuan, Thermal conductivity of microPCMs-filled epoxy matrix composites, Colloid and Polymer Science, Vol.289 (2011), pp.1535-1542

[28] S. Marchi, S. Pagliolico, G. Sassi, Characterization of panels containing micro-encapsulated Phase Change Materials, Energy Conversion and Management, Vol. 74 (2013), pp.261-268

[29] M. Karkri, M. Lachheb, Z. Nógellová, B. Boh, B. Sumiga, M.A. AlMaadeed, A. Fethi, I. Krupa, Thermal properties of phase-change materials based on high-density polyethylene filled with micro-encapsulated paraffin wax for thermal energy storage, Energy and Buildings, Vol.88 (2015), pp.144-152

[30] The Japan Society of Mechanical Engineers ed., JSME Data Handbook: Heat Transfer 5th Edition, The Japan Society of Mechanical Engineers, Tokyo, 2009, pp.52-53 (in Japanese)

Figures Legends

Fig. 1: Microencapsulated PCM and PCM master batch. (a) Microencapsulated PCM. (b) PCM master batch.

Fig. 2: Aluminum mold and stainless steel plate.

Fig. 3: PCM sheet.

Fig. 4: Test section in experiment on thermal performance of PCM sheets. (a) General view. (b) Cross-sectional view.

Fig. 5: Fitting curve and the definition of maximum temperature rise and saturation time. (a) Case temperature without PCM sheet. (b) Case temperature when using PCM sheet C (9.86 g).

Fig. 6: Relationship between temperature rise and time. (a) Heater temperature. (b) Case temperature.

Fig. 7: Relationship between mass of PCM master batch and saturation time.

Fig. 8: Manufacturing method of modified PCM sheet.

Fig. 9: Modified PCM sheet.

Fig. 10: Test section of the experiment on the application of the PCM sheet to the smart phone simulator. (a) Dimensions. (b) Thermocouple locations. (c) Cross-sectional view.

Fig. 11: Relationship between temperature rise and time. (a) Heater temperature. (b) Front case temperature.

Fig. 12: Maximum temperature rise at different conditions. (a) Heater temperature. (b) Front case temperature.

Fig. 13: Saturation time at different conditions. (a) Heater temperature. (b) Front case temperature.

Fig. 14: Finite element model.

Fig. 15: Comparison between solid model and phase change model (L = 0 J/kg, μ = 1 Pa·s) with PE sheet. (a) Solid model. (b) Phase change model (L = 0 J/kg, μ = 1 Pa·s).

Fig. 16: Comparison between numerical results and experimental results. (a) No sheet. (b) PE sheet (25×25×4 mm). (c) PCM sheet (25×25×4 mm). (d) PCM sheet (50×50×1 mm).

Tables Legends

Table 1: Physical properties of microencapsulated PCM.

Table 2: Dimensions and mass of PCM sheets.

Table 3: Physical properties used in the simulation.

Table 4: Estimated physical properties of PCM sheet.

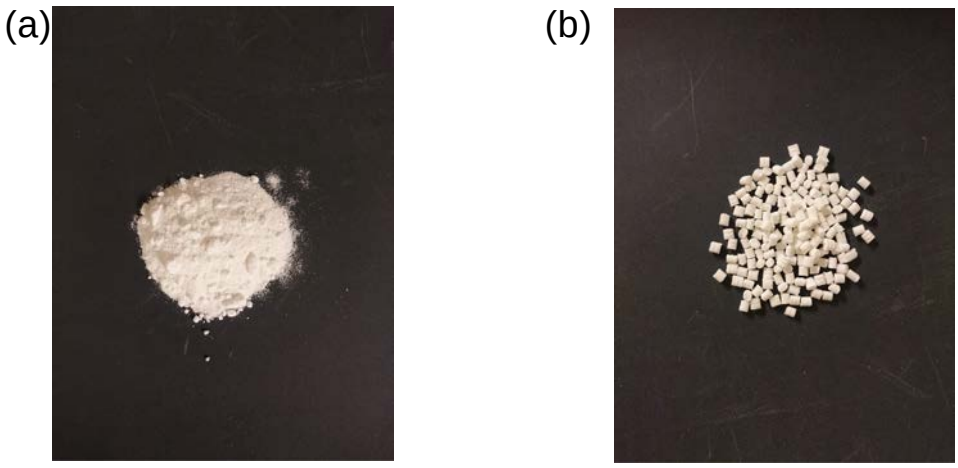

Fig. 1 Microencapsulated PCM and PCM master batch. (a) Microencapsulated PCM. (b) PCM master batch.

Fig. 2 Aluminum mold and stainless steel plate.

Fig. 3 PCM sheet.

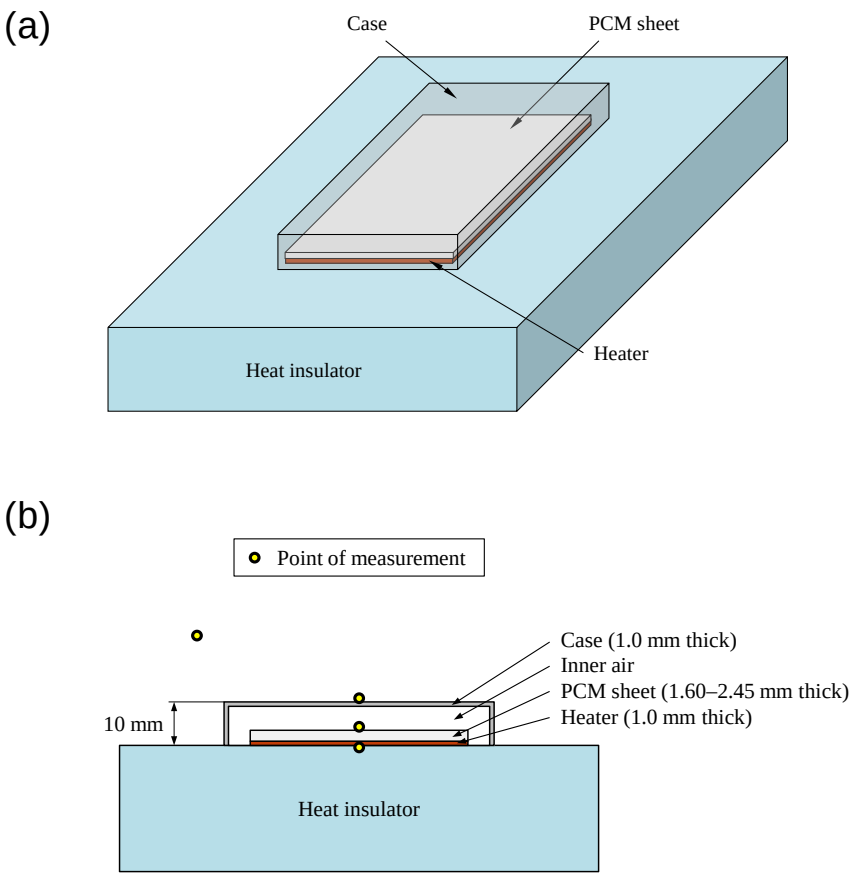

Fig. 4 Test section in experiment on thermal performance of PCM sheets. (a) General view. (b) Cross-sectional view.

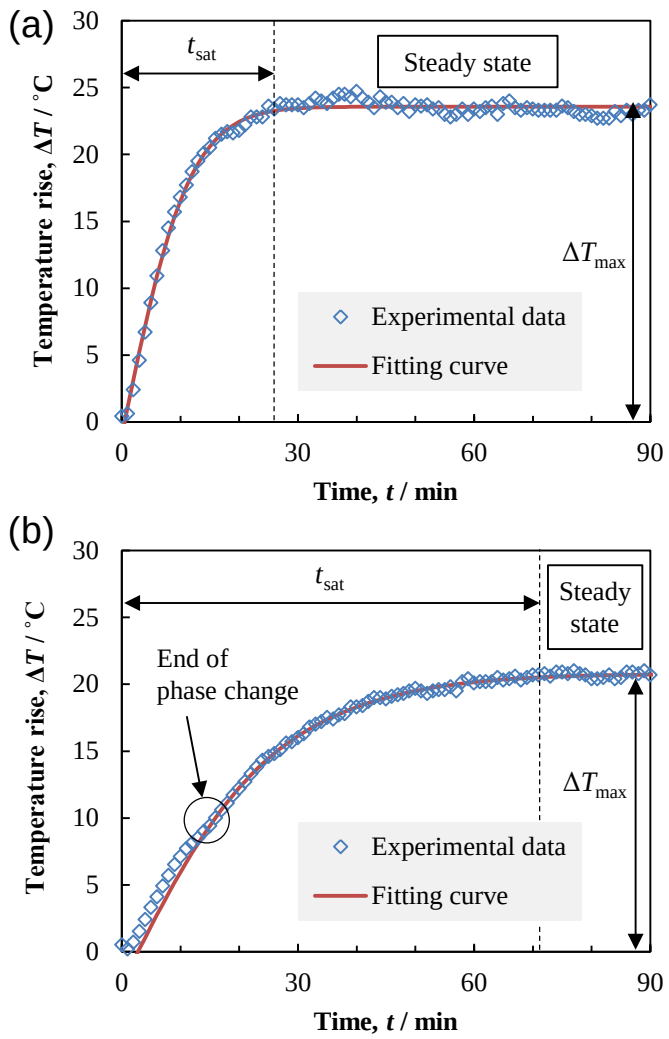

Fig. 5 Fitting curve and the definition of maximum temperature rise and saturation time. (a) Case temperature without PCM sheet. (b) Case temperature when using PCM sheet C (9.86 g).

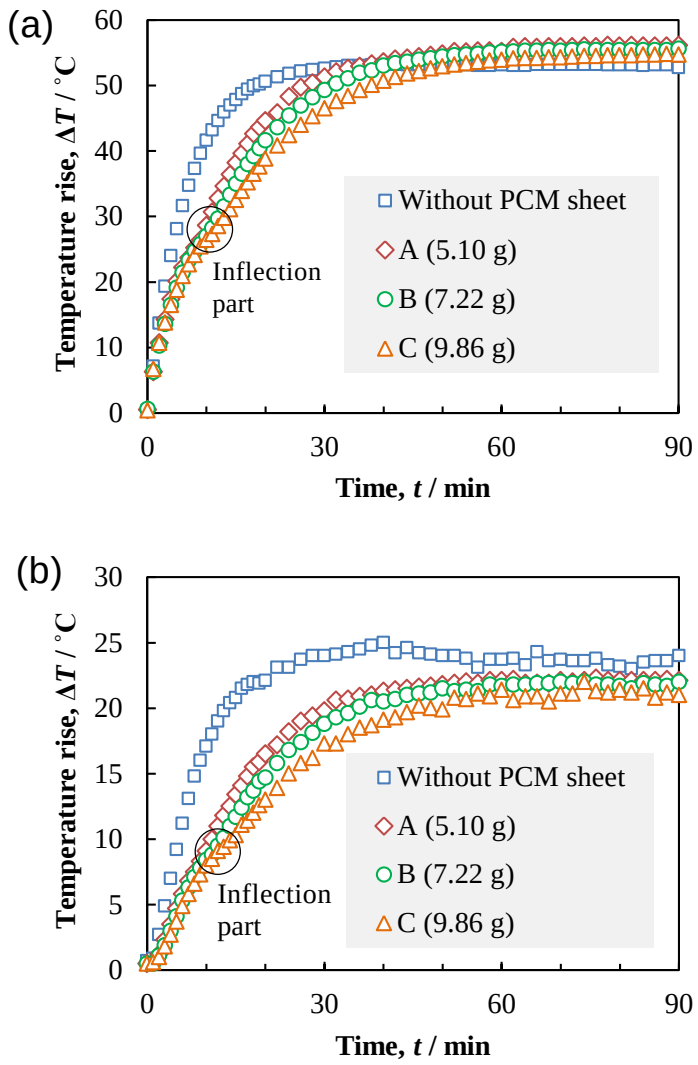

Fig. 6 Relationship between temperature rise and time. (a) Heater temperature. (b) Case temperature.

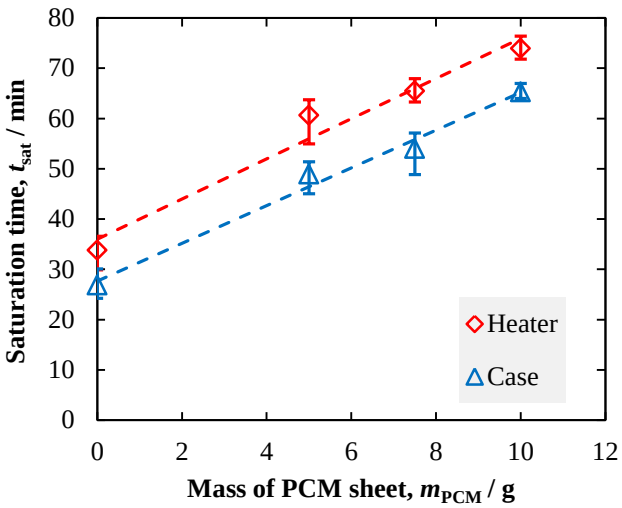

Fig. 7 Relationship between mass of PCM master batch and saturation time.

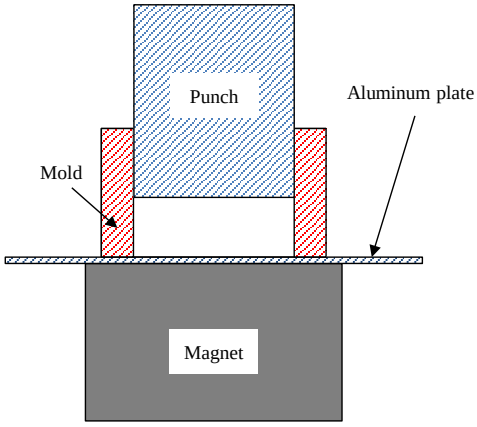

Fig. 8 Manufacturing method of modified PCM sheet.

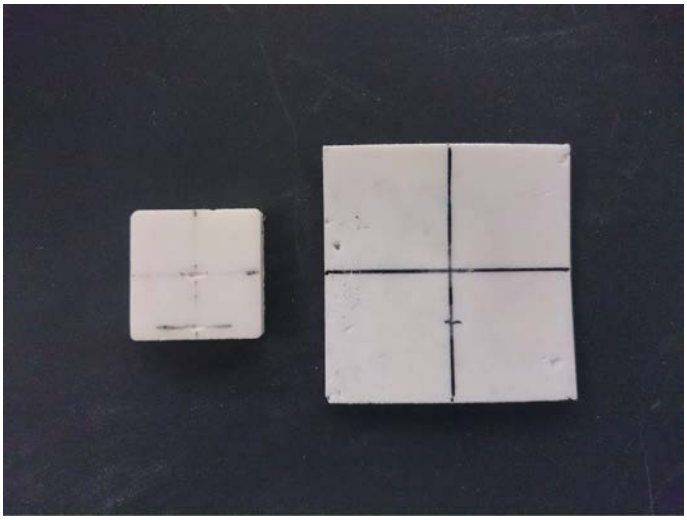

Fig. 9 Modified PCM sheet.

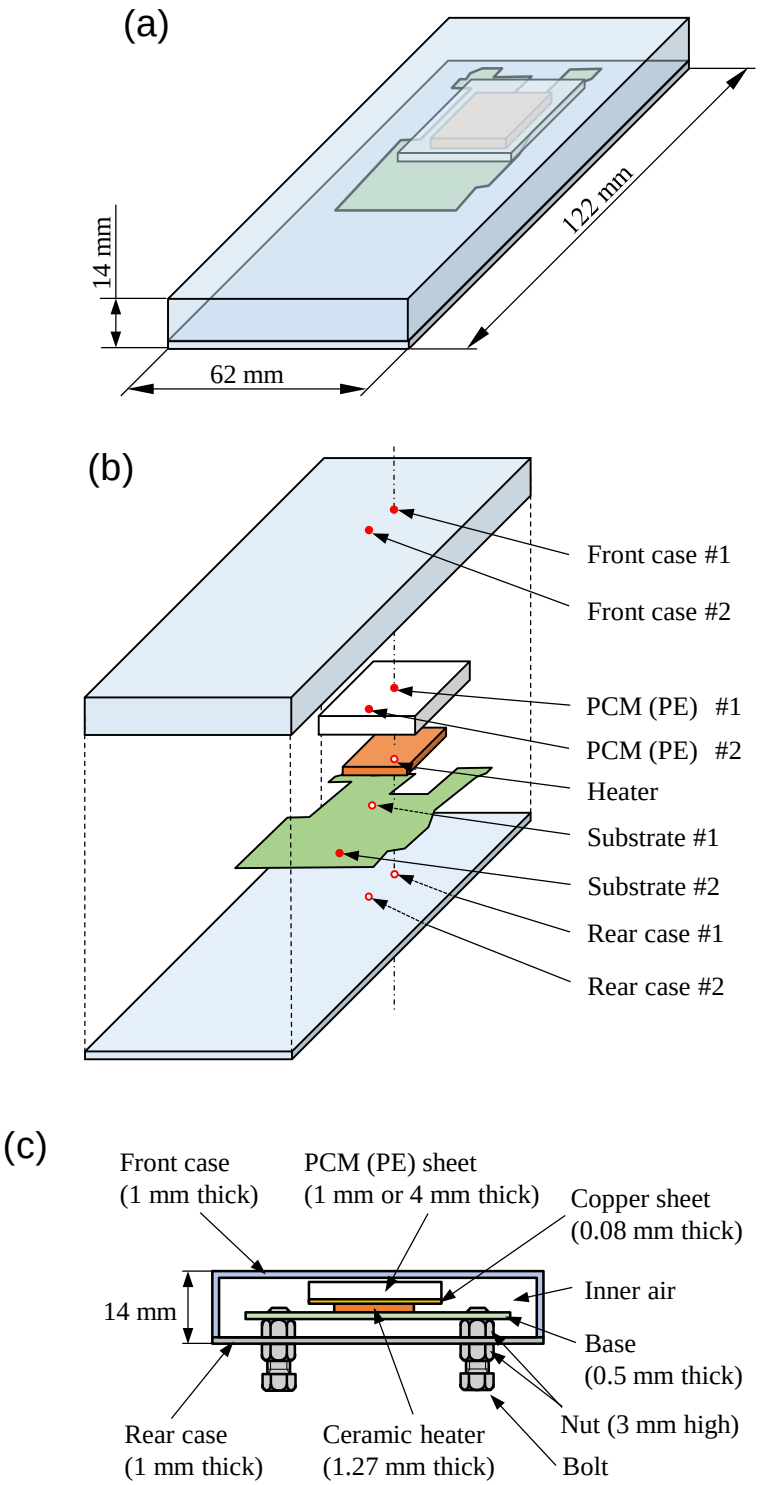

Fig. 10 Test section of the experiment on the application of the PCM sheet to the smart phone simulator. (a) Dimensions. (b) Thermocouple locations. (c) Cross-sectional view.

(a)

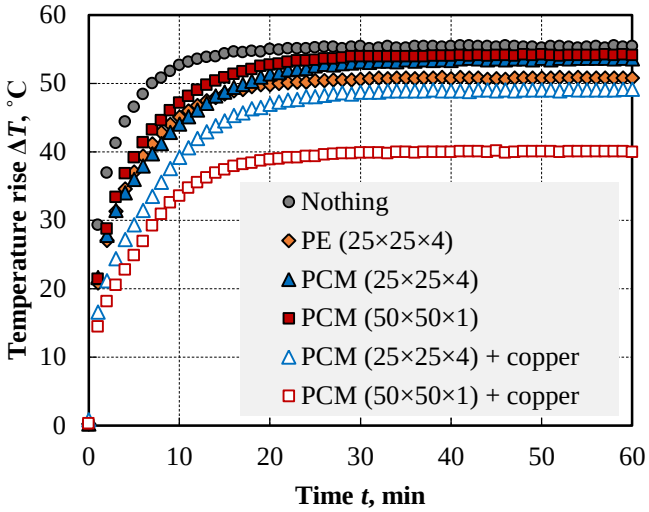

(b)

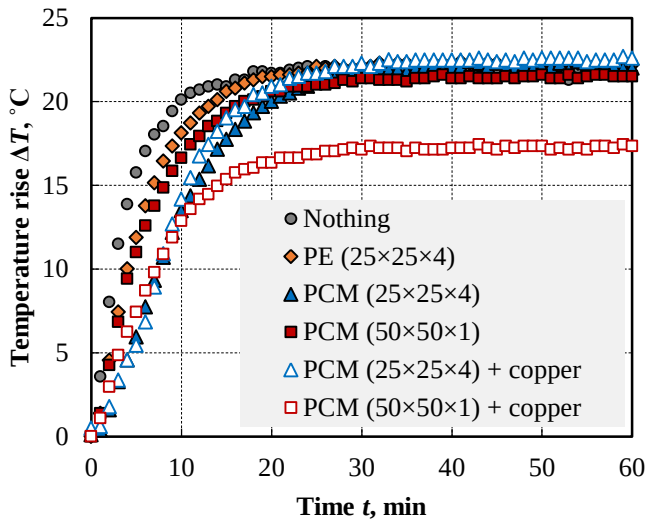

Fig. 11 Relationship between temperature rise and time. (a) Heater temperature. (b) Front case temperature.

(a)

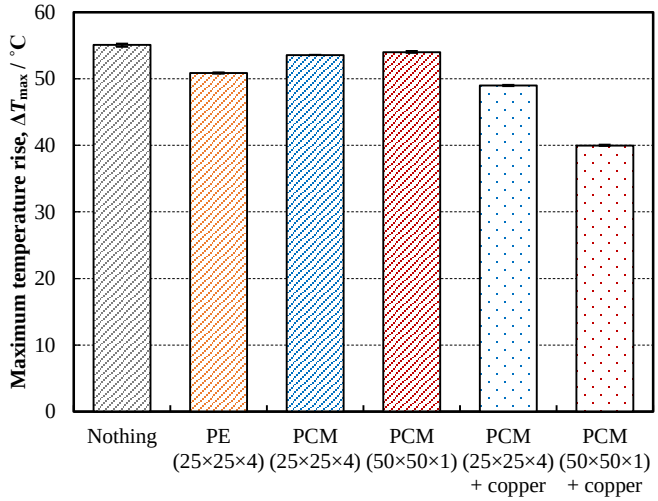

(b)

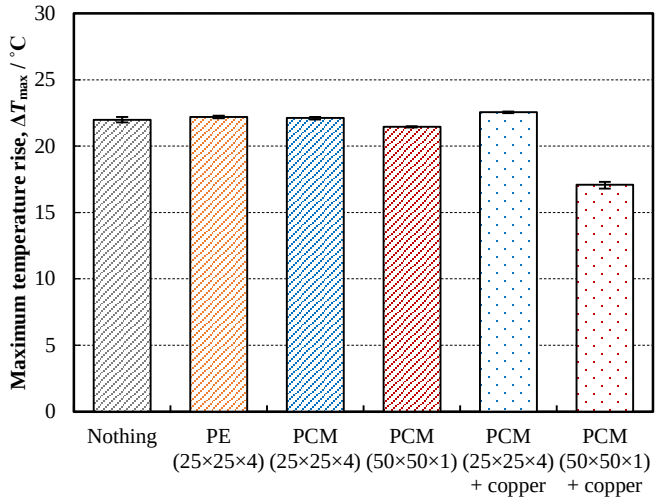

Fig. 12 Maximum temperature rise at different conditions. (a) Heater temperature. (b) Front case temperature.

(a)

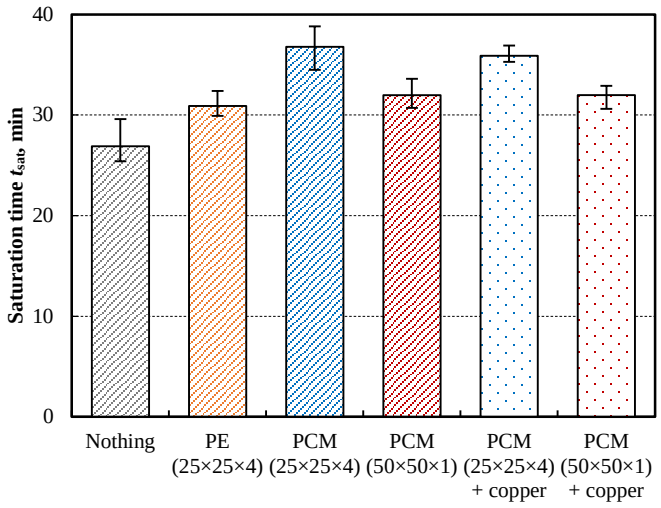

(b)

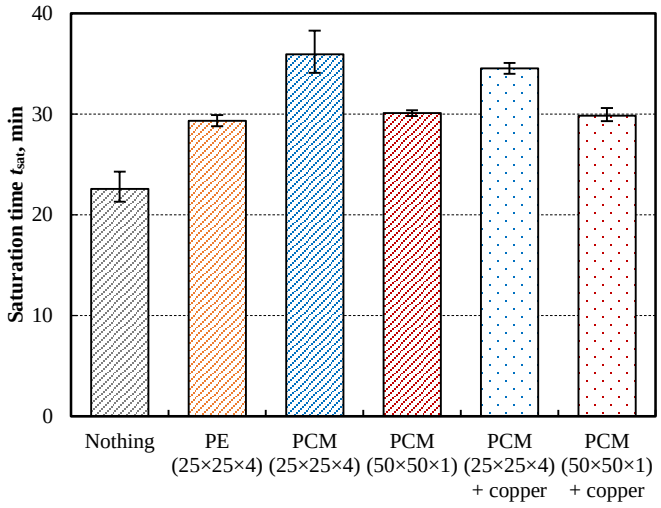

Fig. 13 Saturation time at different conditions. (a) Heater temperature. (b) Front case temperature.

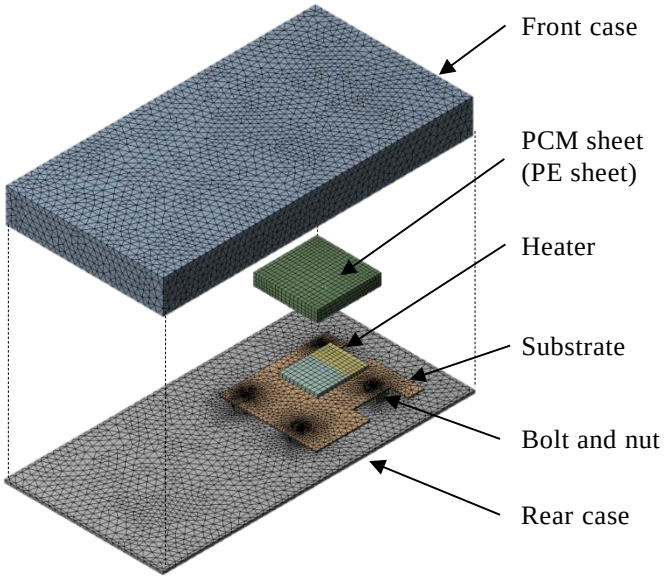

Fig. 14 Finite element model.

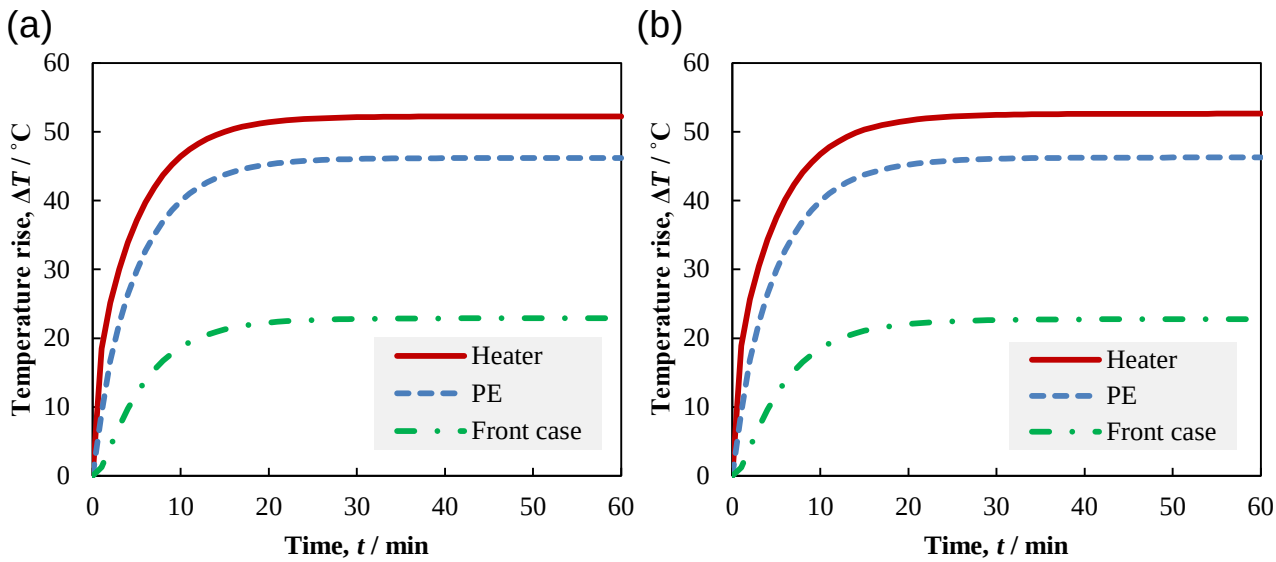

Fig. 15 Comparison between solid model and phase change model (L = 0 J/kg, μ = 1 Pa·s) with PE sheet. (a) Solid model. (b) Phase change model (L = 0 J/kg, μ = 1 Pa·s).

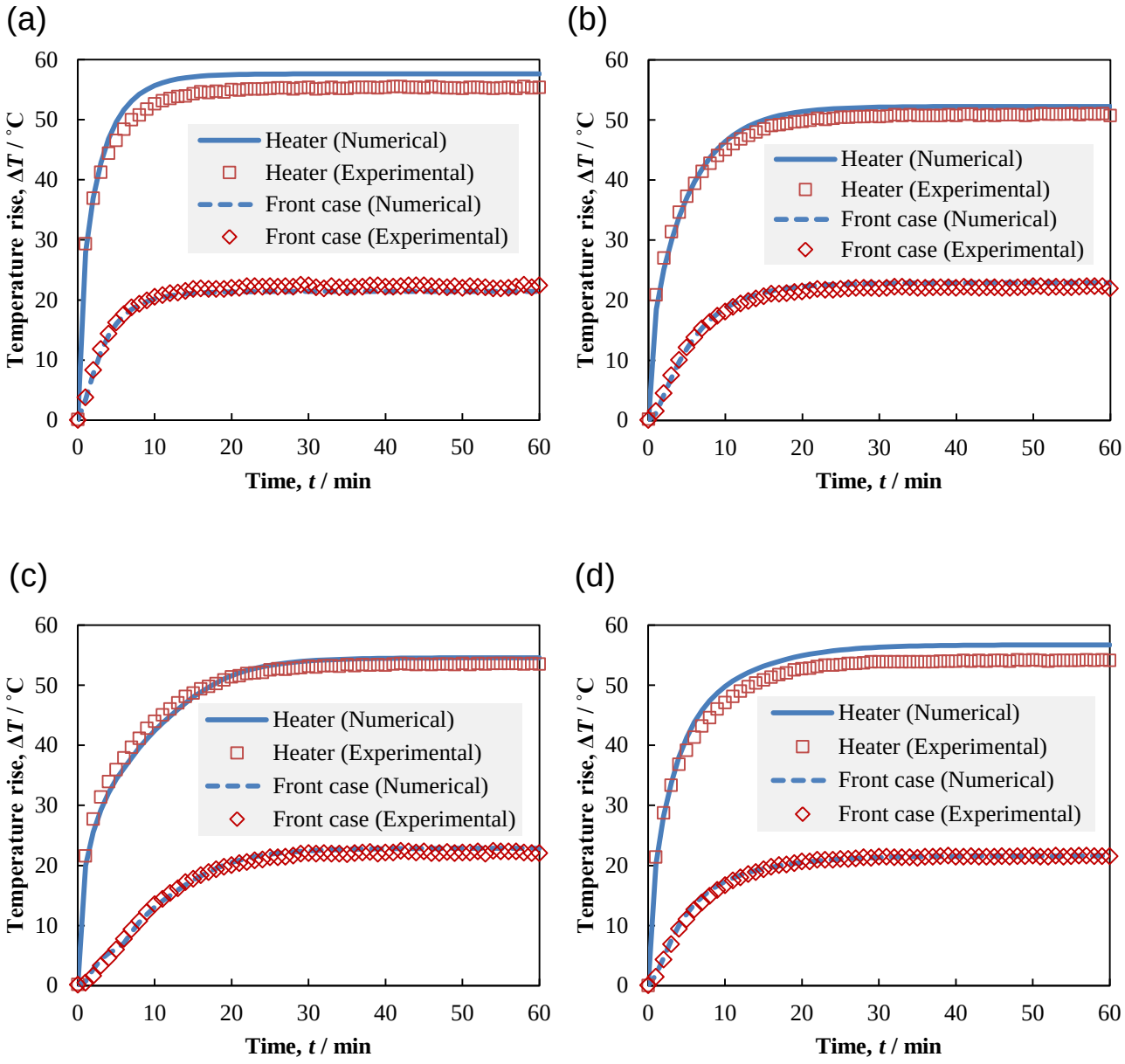

Fig. 16 Comparison between numerical results and experimental results. (a) No sheet. (b) PE sheet (25×25×4 mm). (c) PCM sheet (25×25×4 mm). (d) PCM sheet (50×50×1 mm).

Table 1 Physical properties of microencapsulated PCM.

	Melting point [°C]	Latent heat [kJ/kg]	Specific heat [kJ/kg·K]	Bulk density [kg/m^3]
PMCD-32SP	32	140-160	1.6	300-600

Table 2 Dimensions and mass of PCM sheets.

	Dimensions			Mass [g]
	Length [mm]	Width [mm]	Thickness [mm]	
PCM sheet A	100	50	1.60	5.10
PCM sheet B	100	50	2.10	7.22
PCM sheet C	100	50	2.45	9.86

Table 3 Physical properties used in the simulation.

Parts	Materials	Density [kg/m^3]	Specific heat [kJ/kg·K]	Thermal conductivity [W/m·K]	Emissivity
Front case	Polycarbonate	1200	1.20	0.19	0.9
Rear case	Acylic	1190	1.47	0.21	0.9
Substrate	Epoxy and copper	3690	0.880	25 0.5 (Thickness direction)	0.7
Heater	Ceramic	3890	0.780	18	0.7
PE sheet	Polyethylene	953	1.89	0.5	0.9
Bolt and nut	Steel	7830	0.461	16.3	0.7
Thermal tape	–	3900	0.800	0.5	–

Table 4 Estimated physical properties of PCM sheet.

Density [kg/m^3]	Specific heat [kJ/kg·K]	Thermal conductivity [W/m·K]	Emissivity
846	1.97	0.26	0.9

Latent heat [kJ/kg]	Melting temperature [°C]	Solidus temperature [°C]	Liquidus temperature [°C]
86.7	32	31	33